



Shadow of the Kerr–Newman–Kiselev–Letelier Black Hole

Yovqochev Pahlavon Navruzovich

National University of Uzbekistan

Dilmurod Ortiqboyev

Gulistan state University

Annotation: In this research, we examine shadow formation of the Kerr–Newman–Kiselev–Letelier (KNKL) black hole. We investigate these phenomena for different values of the spacetime parameters, including the quintessence parameter γ , the cloud of string (CS) parameter b , the spin parameter a , and the charge Q of the black hole. We also examine the emission energy rate from the KNKL black hole. Lastly, we explore the impact of plasma on photon motion, shadow size, and shape of the KNKL black hole.

Keywords: Kerr–Newman–Kiselev–Letelier (KNKL) black hole, shadow, gravity, plasma.

I. Introduction

To investigate gravity in the strong field regime, black holes can serve as a testing ground. The behavior of particles near black holes provides valuable insights into the structure of spacetime. According to General Relativity (GR), the bending of light by a gravitational source leads to the formation of a black hole shadow. Analyzing the paths of photons, known as null geodesics, in the spacetime is crucial for studying the black hole shadow. The presence of light rings, which are circular orbits followed by photons near black holes, results in the appearance of a dark disc in the sky known as the black hole shadow. The concept of observing the black hole shadow was initially proposed by Falcke et al. [1]. Two key parameters characterizing astrophysical black holes are their mass and spin. Mass estimation has been resolved, leading to the classification of black holes into stellar, intermediate, supermassive, and miniature types [2]. However, determining the spin of rotating black holes is still an ongoing endeavor, and studying black hole shadows is believed to aid in this process [3]. Recent developments, such as the observation of gravitational waves from merging black holes [4], the imaging of the shadow of the central supermassive black hole in the Messier 87 (M87*) galaxy [5], and the Milky Way galaxy [6], have further intensified interest in exploring black hole spacetimes.

II. Null geodesics in the Kerr–Newman–Kiselev–Letelier black hole

The KNKL black hole metric is given by

$$ds^2 = -\frac{\Delta}{\Sigma} (dt - a \sin^2 \theta d\phi)^2 + \frac{\Sigma}{\Delta} dr^2 + \Sigma d\theta^2 + \frac{\sin^2 \theta}{\Sigma} (adt - (r^2 + a^2)d\phi)^2 \quad (1)$$

Where the metric coefficients of (1) are

$$\Sigma = r^2 + a^2 \cos^2 \theta, \quad (2)$$



$$\Delta = (1 - b)r^2 + a^2 + Q^2 - 2Mr - \gamma r^{-2\omega_q+1} \quad (3)$$

When $\Delta=0$, the horizon of the black hole spacetime can be determined. By solving $\Delta=0$ numerically, Fig. 1 illustrates the behavior of the horizon radius for different values of γ and b , while a and Q are fixed for the KNKL black hole. The figure indicates that the horizon radius of the KNKL black hole increases as γ and b values increase, resulting in a smaller horizon radius compared to the Kerr black hole. For further insights into the horizon structure of the KNKL black hole, refer to [7]. To determine the shadow shape cast by the KNKL black hole, we examine null geodesics using the Hamilton-Jacobi formalism in the KNKL black hole spacetime, as described in [8].

$$\frac{\partial S}{\partial \tau} = -\frac{1}{2} g^{\mu\nu} \frac{\partial S}{\partial x^\mu} \frac{\partial S}{\partial x^\nu}, \quad (4)$$

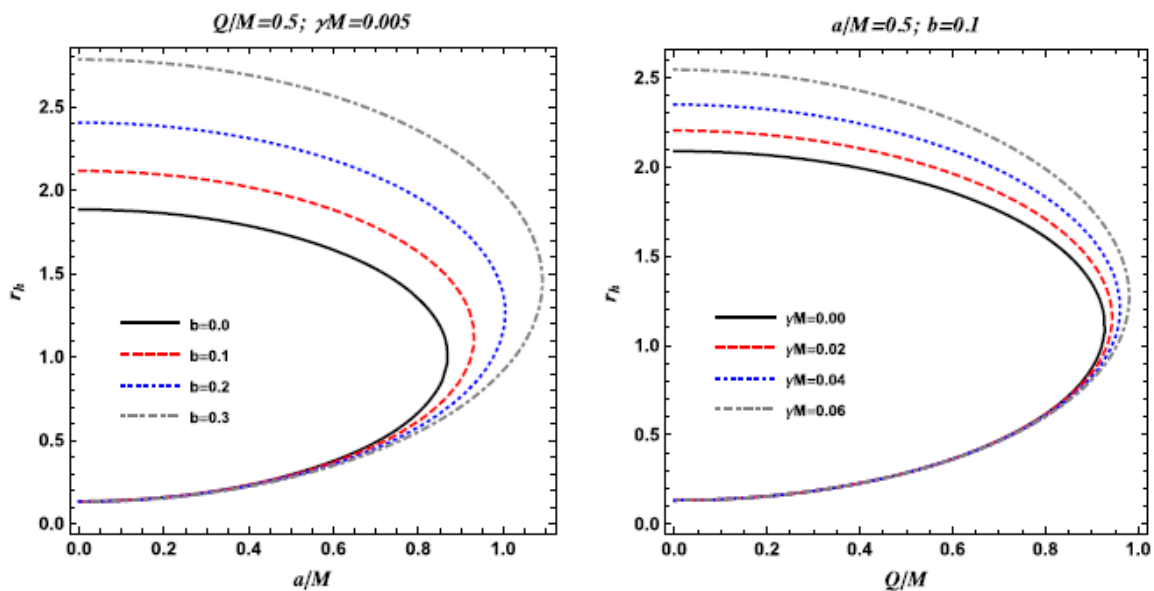


Fig. 1. The horizons of the KNKL black hole

$$S = \frac{1}{2} m_0^2 \tau - Et + L_z \phi + S_r(r) + S_\theta(\theta), \quad (5)$$

where m_0 is the mass of the particle and $S_r(r)$, $S_\theta(\theta)$ are the function of r and θ only. The equations for the motion of a photon in the space-time metric of the KNKL black hole are obtained by using the method of separation of variables and assuming the mass of the particle ($m_0 = 0$)

$$\mathcal{R} = [(r^2 + a^2)E - aL_z]^2 - \Delta[\mathcal{K} + (L_z - aE)^2], \quad (6)$$

$$\Theta = \mathcal{K} + \cos^2 \theta (a^2 E^2 - L_z^2 \sin^{-2} \theta). \quad (7)$$

$$\Sigma \frac{dt}{d\tau} = a(L_z - aE \sin^2 \theta) + \frac{r^2 + a^2}{\Delta} (E(r^2 + a^2) - aL_z), \quad (8)$$

$$\Sigma \frac{dr}{d\tau} = \pm \sqrt{\mathcal{R}} \quad (9)$$



$$\Sigma \frac{d\theta}{d\tau} = \pm\sqrt{\Theta} \quad (10)$$

$$\Sigma \frac{d\phi}{d\tau} = (L_z \csc^2 \theta - aE) + \frac{a}{\Delta} (E(r^2 + a^2) - aL_z) \quad (11)$$

By considering the geodesic equation involving the radial coordinate \dot{r} , we can derive the boundary of the shadow cast by the KNKL black hole

$$\left(\Sigma \frac{dr}{d\tau}\right)^2 + V_{eff} = 0 \quad (12)$$

The effective potential in the equatorial plane ($\theta = \pi/2$) is

$$V_{eff} = \frac{\Delta(\mathcal{K} + (L_z - aE)^2) - ((a^2 + r^2)E - aL_z)^2}{2r^4} \quad (13)$$

Figure 2 illustrates the general behavior of the effective potential with respect to the radial coordinate (r) for various values of the CS parameter (b) and the quintessence parameter (γ), while keeping the spin and charge of the KNKL black hole constant.

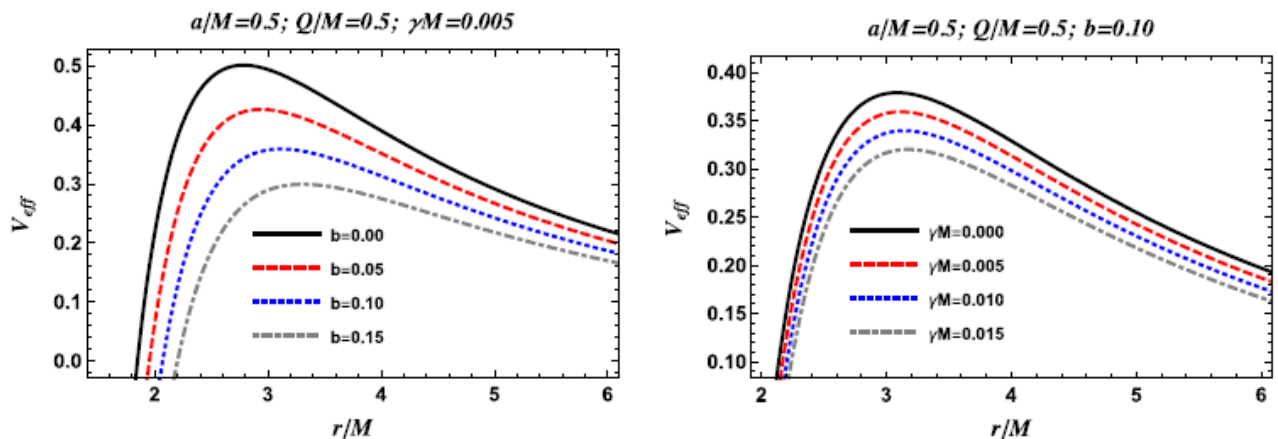


Fig. 2 Effective potential around KNKL black hole for the massless particle

III. Rate of emission energy

Due to quantum fluctuations near the horizon of a black hole, particle pairs are created and annihilated. Positive energy particles can escape through quantum tunneling, causing the black hole to radiate energy known as Hawking radiation. When the black hole approaches a limiting constant value σ_{lim} at high energy, the absorption cross section of the black hole undergoes slight modulation. This leads to the observer at infinity perceiving a variation in the high energy absorption cross section due to the shadow cast by the black hole. The limiting constant value σ_{lim} , which is connected to the radius of the photon sphere, can be obtained as [9,10].

$$\sigma_{lim} \approx \pi R_{sh}^2 \quad (14)$$

The emission rate varies with the frequency ω , and increasing the parameters b and γ leads to a higher peak in the emission rate graph, indicating a slower evaporation process for lower energy emissions.



$$\sigma_{lim} \approx \pi R_{sh}^2 \quad (14)$$

The rate of the energy emission

$$\frac{d^2 \varepsilon}{d\omega dt} = \frac{2\pi^2 \sigma_{lim}}{e^{\frac{\omega}{T}} - 1} \omega^3. \quad (15)$$

The Hawking temperature $T = \kappa/2\pi$ represents the expression for the surface gravity denoted by κ . By combining Equation (14) with Equation (15), we obtain an alternative form for the emission energy rate expression.

$$\frac{d^2 \varepsilon}{d\omega dt} = \frac{2\pi^3 R_{sh}^2}{e^{\frac{\omega}{T}} - 1} \omega^3. \quad (16)$$

Figure 3 illustrates the variation of the energy emission rate concerning the photon frequency ω , considering fixed values of the black hole's spin a and charge Q , along with different values of parameters b and γ . The graph shows that increasing the values of b and γ enhances the peak of the energy emission rate, suggesting a slower evaporation process for the black hole at lower energy emission rates.

IV. Dynamics of photon in plasma medium

In this scenario, we employ the Hamiltonian to describe the motion of a light ray circling a black hole that is enveloped by plasma. From this, we derive the equation of motion in the given form:

$$\mathcal{H} = \frac{1}{2} [g^{\mu\nu} p_\mu p_\nu + \omega_p(x)^2], \quad (17)$$

The electron plasma frequency, denoted as ω_p , is defined as part of this formulation.

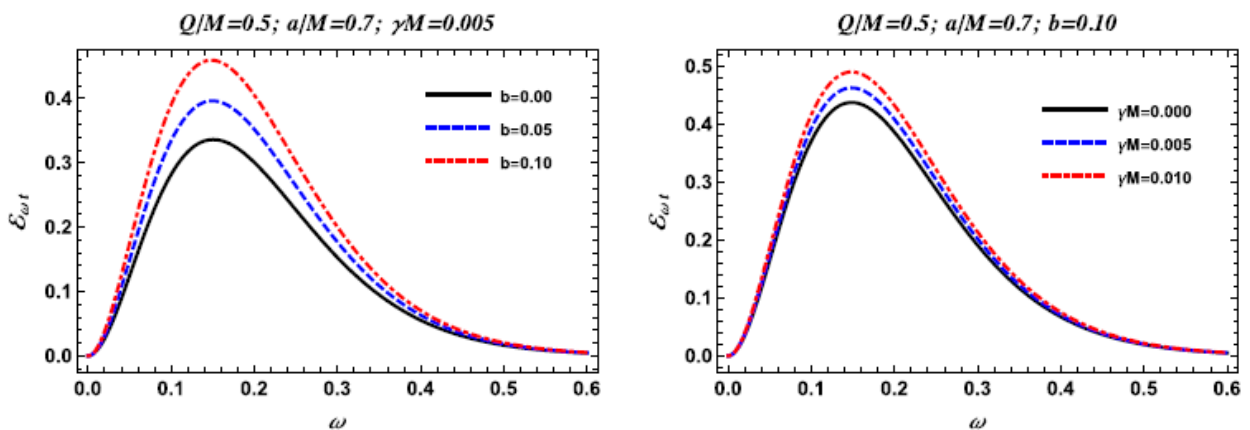


Fig. 3 The emission energy

$$\omega_p(x)^2 = \frac{4\pi e^2}{m_e} N_e(x), \quad (18)$$

With the electron's charge (e) and mass m_e , and the number density of electrons (N_e) we can describe the Hamilton-Jacobi equation for photons



$$\mathcal{H}\left(x, \frac{\partial S}{\partial x}\right) = 0 \quad (19)$$

By employing the method of separation of variables, we can express the action in a separable form

$$S = -\omega_0 t + p_\phi \phi + S_r(r) + S_\theta(\theta), \quad (20)$$

where the conserved quantities are the particle's angular momentum p_ϕ , and energy ω_0 . Recent studies have shown that the plasma frequency in the rotating black hole can be represented using certain functions $h(r)$ and $g(\theta)$ related to the radial and angular components.

$$\omega_p(x)^2 = \frac{h(r) + g(\theta)}{\rho}, \quad (21)$$

By substituting equations (20) and (21) into equation (19), we obtain the following expression

$$0 = \frac{a^2 \Delta \sin^2 \theta - (r^2 + a^2)^2}{\Delta} \omega_0^2 + \frac{4aMre^{-\frac{l}{r}}}{\Delta} \omega_0 p_\phi + \Delta(S'_r)^2 + (S'_\theta)^2 + \frac{\Delta - a^2 \sin^2 \theta}{\Delta \sin^2 \theta} p_\phi^2 + h(r) + g(\theta), \quad (22)$$

In the KNKL black hole spacetime with a plasma medium, we utilize the Carter constant (\mathcal{K}) to separate the equation into two parts, as described in reference [11]

$$(S'_\theta)^2 + \left(a\omega_0 \sin \theta - \frac{p_\phi}{\sin \theta}\right)^2 + g(\theta) = \mathcal{K} \quad (23)$$

$$\frac{1}{\Delta} - \Delta(S'_r)^2 \left((r^2 + a^2)\omega_0 - ap_\phi\right)^2 - h(r) = \mathcal{K} \quad (24)$$

By using equation (22), we can derive the equation of motion in the spacetime of the KNKL black hole with a plasma medium

$$\rho^2 \frac{dt}{d\tau} = a(p_\phi - a\omega_0 \sin^2 \theta) + \frac{r^2 + a^2}{\Delta} P(r), \quad (25)$$

$$\rho^2 \frac{dr}{d\tau} = \pm \sqrt{\mathcal{R}}, \quad (26)$$

$$\rho^2 \frac{d\theta}{d\tau} = \pm \sqrt{\Theta}, \quad (27)$$

$$\rho^2 \frac{d\phi}{d\tau} = \frac{p_\phi}{\sin^2 \theta} - a\omega_0 + \frac{a}{\Delta} P(r) \quad (28)$$

where $P(r)$ is given by

$$P(r) = (r^2 + a^2)\omega_0 - ap_\phi \quad (29)$$

The functions \mathcal{R} and Θ correspond to the radial and angular equations of motion, respectively.



$$\mathcal{R} = P(r)^2 - \Delta \left[Q + (p_\phi - a\omega_0)^2 + h(r) \right], \quad (30)$$

$$\Theta = Q + \cos^2 \theta \left(a^2 \omega^2 - p_\phi^2 \sin^{-2} \theta \right) - g(\theta), \quad (31)$$

$$Q = \mathcal{K} - (p_\phi - a\omega_0)^2.$$

Shadow of the Kerr–Newman–Kiselev–Letelier black hole in the presence of plasma

To analyze the shadows of black holes, we examine the boundary of circular light rays using the conditions $\mathcal{R} = \mathcal{R}' = 0$. These conditions yield constants of motion in terms of the radius (r) of the circular photon orbits [11].

$$Q = \frac{(ap_\phi - \omega_0(a^2 + r^2))^2}{\Delta} - (p_\phi - a\omega_0)^2 - h(r), \quad (32)$$

$$p_\phi = \frac{\omega_0}{a} \left[r^2 + a^2 - \frac{\Delta}{a\Delta'} \left(\sqrt{4r^2 - \frac{h'(r)\Delta'(r)}{\omega_0}} + 2r \right) \right] \quad (33)$$

Then, employing celestial coordinates, we depict the silhouette of the black hole's shadow in the presence of plasma. The representation takes the following

$$\alpha = -\frac{p_\phi}{\omega_0 \sin \theta_0} \sqrt{f(r_0)} \quad (34)$$

$$\beta = \pm \frac{\sqrt{f(r_0)}}{\omega_0} \sqrt{Q + \cos^2 \theta \left(a^2 \omega^2 - \frac{p_\phi^2}{\sin^2 \theta_0} \right) - g(\theta_0)}. \quad (35)$$

We consider the case of dust at rest at infinity to examine the size and shape as functions of spacetime parameters for the plasma in our analysis. However, this plasma distribution does not follow the separable form given by Eq. (21). Hence, following [11], we introduce an additional angular dependency in the frequency by choosing [11]:

$$h(r) = \omega_c^2 \sqrt{M^3 r}, \quad (36)$$

$$g(\theta) = 0, \quad (37)$$

$$\omega_p^2 = \omega_c^2 \frac{\sqrt{M^3 r}}{r^2 + a^2 \cos^2 \theta}, \quad (38)$$

where ω_c is a constant and M represents the black hole's mass. By combining Eqs. (34)-(37) in the equatorial plane, we obtain the shadow cast by the KNKL black hole. The plots in Figure 4 illustrate the black hole's shadow for various values of spacetime and plasma parameters.

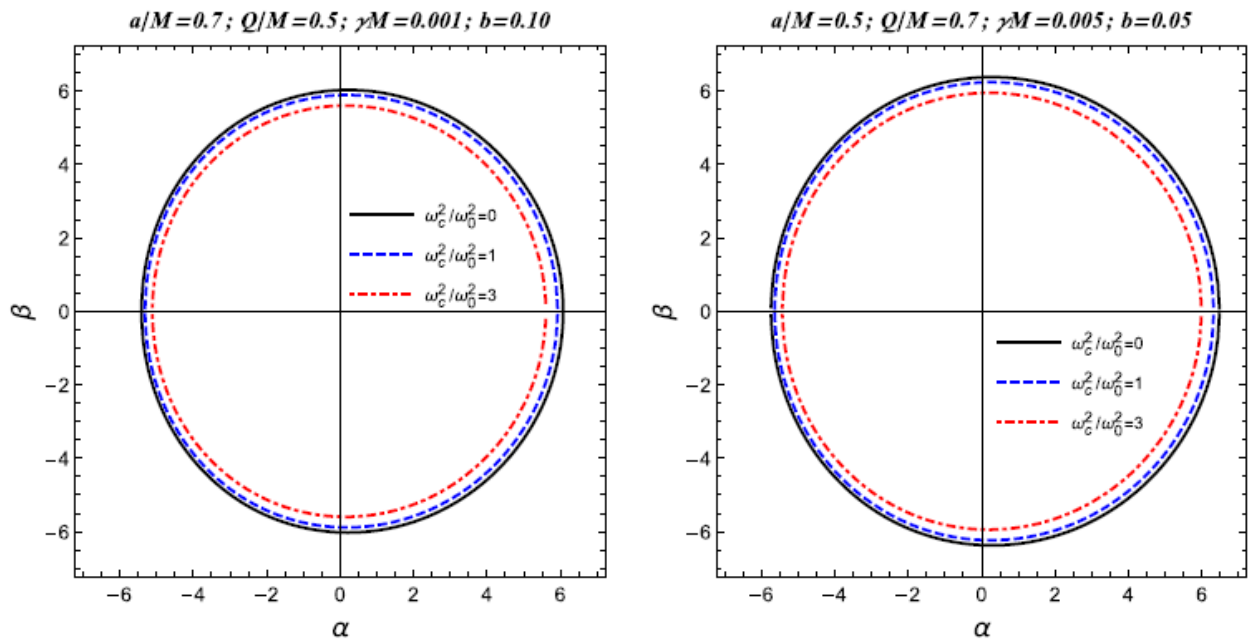
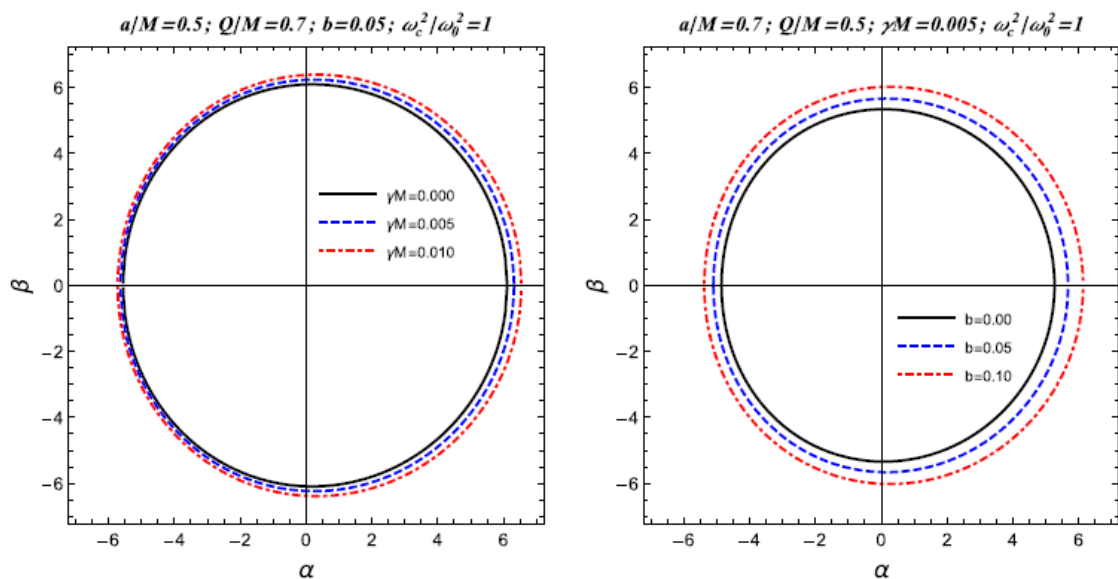


Fig. 4. The black hole shadow in plasma

V. Conclusion and discussions

Our findings indicate that increasing values of γ and b lead to larger shadows and stronger gravitational fields of the KNKL black hole. Conversely, an increase in the black hole's charge Q results in a smaller shadow. Additionally, higher values of the spin parameter a cause more significant distortion in the black hole's shadow. When keeping the spacetime parameters constant, we find that a stronger plasma medium leads to a smaller shadow and a decreased intensity of the KNKL black hole's gravitational field in the presence of plasma.



References

1. H. Falcke, F. Melia, E. Agol, *ApJ* **528**, L13 (2000). <https://doi.org/10.1086/312423>. arXiv:astro-ph/9912263
2. W.M. Farr et al., *Astrophys. J.* **741**, 103 (2011).



- <https://doi.org/10.1088/0004-637X/741/2/103>. arXiv:1011.1459
3. R. Takahashi, ApJ **611**, 996 (2004).
<https://doi.org/10.1086/422403>. arXiv:astro-ph/0405099
 4. B.P. Abbott et al., Phys. Rev. Lett **116**, 061102 (2016).
<https://doi.org/10.1103/PhysRevLett.116.061102>. arXiv:1602.03837 [grqc]
 5. K. Akiyama et al., ApJ **875**, L1 (2019).
<https://doi.org/10.3847/2041-8213/ab0ec7>. arXiv:1906.11238 [astro-ph.GA]
 6. K. Akiyama et al., Astrophys. J. Lett **930**, L12 (2022).
<https://doi.org/10.3847/2041-8213/ac6674>
 7. J.M. Toledo, V.B. Bezerra, Gen. Relativ. Gravit. **52**, 34 (2020).
<https://doi.org/10.1007/s10714-020-02683-1>
 8. B. Carter, Phys. Rev. **174**, 1559 (1968).
<https://doi.org/10.1103/PhysRev.174.1559>
 9. S.-W. Wei, Y.-X. Liu, J. Cosmol. A. P. **2013**, 063 (2013).
<https://doi.org/10.1088/1475-7516/2013/11/063>. arXiv:1311.4251 [grqc]
 10. F. Atamurotov, U. Papnoi, K. Jusufi, Class. Quantum Gravity **39**, 025014 (2022).
<https://doi.org/10.1088/1361-6382/ac3e76>. arXiv:2104.14898 [gr-qc]
 11. J. Badía, E.F. Eiroa, Phys. Rev. D **104**, 084055 (2021).
<https://doi.org/10.1103/PhysRevD.104.084055>. arXiv:2106.07601 [gr-qc]